Evaporation-condensation transition of the two-dimensional Potts model in the microcanonical ensemble

Tomoaki Nogawa* and Nobuyasu Ito
Department of Applied Physics, The University of Tokyo, Hongo, Bunkyo-ku, Tokyo 113-8656, Japan

Hiroshi Watanabe
Institute for Solid State Physics, The University of Tokyo, Kashiwanoha 5-1-5, Kashiwa, Chiba 277-8581, Japan
(Received 5 September 2011; published 5 December 2011)

The evaporation-condensation transition of the Potts model on a square lattice is numerically investigated by the Wang-Landau sampling method. An intrinsically system-size-dependent discrete transition between supersaturation state and phase-separation state is observed in the microcanonical ensemble by changing constrained internal energy. We calculate the microcanonical temperature, as a derivative of microcanonical entropy, and condensation ratio, and perform a finite-size scaling of them to indicate the clear tendency of numerical data to converge to the infinite-size limit predicted by phenomenological theory for the isotherm lattice gas model.

DOI: 10.1103/PhysRevE.84.061107 PACS number(s): 05.50.+q, 64.60.Cn, 64.60.My, 64.60.Q−

I. INTRODUCTION

A first-order transition as a state transformation of substances is observed in our everyday lives, such as evaporation-condensation and melting-freezing. The thermodynamic mechanism of such transition is very clear; a phase transition occurs when the state of the lowest free energy alternates from one thermodynamic state to another by changing a certain environmental parameter. But dynamics of the transition is rather complicated, and our knowledge cannot be said to be sufficient. Since the initial and final states are completely different from a second-order transition, nucleation and large-scale domain growth, i.e., invasion of the metastable state by the most stable state, is observed in the vicinity of the transition point, which includes various mechanisms depending on the spatiotemporal scale [1–3]. This is essentially nonequilibrium phenomena, and the dynamics is difficult to understand by relating it to the well-understood equilibrium state near the transition point. There is a droplet formation phenomena, however, that can be discussed in an equilibrium framework as mentioned in the following. It can be a good starting point to understand first-order transition dynamics.

In regard to first-order transitions, we usually imagine discontinuous transformation with hysteresis controlled by an intensive variable such as temperature, pressure, and magnetic field. But once we constrain one conjugate extensive variable, such as internal energy, particle density, and magnetization, and take it as a control variable, a coexisting phase is inserted in the phase diagram between two homogeneous phases, and the transitions becomes continuous; the volume fraction of one phase continuously changes from zero to unity between the two edges of the coexisting phase. It is pointed out, however, that a droplet, which is a condensed domain of the minority state in phase separation, is not stable unless its volume is larger than a certain threshold, and therefore there is a discontinuous droplet condensation transition [4,5]. This is basically due to the fact that the surface free energy of the droplet is not negligible in a finite-size system. Therefore the threshold volume of a d-dimensional droplet depends on the system size, proportional to $L^{d^2/(d+1)}$, where L is a linear dimension of the system [6]. Although this threshold can be neglected in comparison with the whole system volume L^d in an infinite-size system, it actually diverges with L. Consequently, the infinite-size limit of the droplet condensation transition is well defined if we observe the phenomena with the proper size scale. It should be noted that equilibrium coexisting states always contain only one large droplet, in contrast with a nonequilibrium transition where multiple droplets appear. The supersaturation state, where condensation is avoided due to small volume of minority state, is related to the metastable state under a fixed intensive parameter condition.

Biskup *et al.* [4] and Binder [5] made quantitative analysis of the equilibrium droplet condensation transition, which is supported by a number of numerical studies of Lenard-Jones particles [7–9] and lattice gas [10–13], where particle-density-driven transitions at given temperature are investigated. In this paper we consider a simpler situation, an internal-energy-driven transition in a microcanonical ensemble [14,15], where density (magnetization) is not explicitly taken account of. By large-scale numerical simulations of the two-dimensional Potts model with the Wang-Landau sampling, we try to determine the large-size limit of the droplet condensation transition, which has been rather difficult in small-size systems [10].

II. MODEL

We investigate the ferromagnetic q-state Potts model [16] on a $L \times L$ square lattice with a periodic boundary condition. The interaction energy with nearest neighbor (NN) couplings is written as

$$E = \sum_{\langle i,j \rangle \in \mathrm{NN}} (1 - \delta_{\sigma_i \sigma_j}), \tag{1}$$

where $\delta_{\alpha\beta}$ means Kronecker's delta and the spin variable σ_i takes an integer value, $1,2,\ldots,q$. This model in a canonical

*nogawa@serow.t.u-tokyo.ac.jp

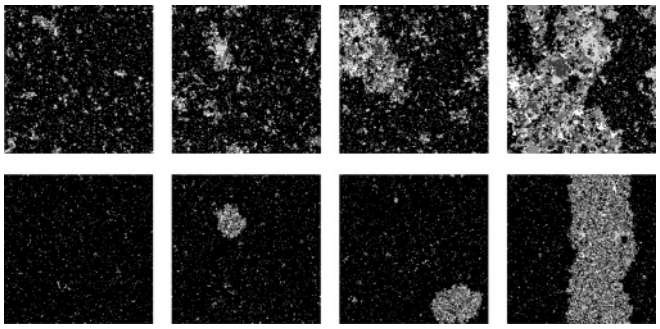

FIG. 1. Typical spin configuration of the system with $q = 8$ (top) and $q = 21$ (bottom) for $L = 256$. The different spin states are denoted by different gray scales. The energy is $E/N = 0.3750, 0.4500, 0.5250$, and 0.7125 (top) and $E/N = 0.1500, 0.2250, 0.2625$, and 0.6750 (bottom) from left to right. The black region is occupied by spins of the most major state, and the dappled gray region is an assemblage of tiny domains with various states.

ensemble exhibits a paramagnetic-ferromagnetic transition at $\beta = \beta_c \equiv \ln(1 + 1/\sqrt{q})$, where $\beta = 1/k_B T$ is the inverse temperature. The transition is of second order for $q \leqslant 4$ and of first order for $q > 4$. When q is not sufficiently larger than 4, the correlation length of fluctuation is considerably large around the transition point, and critical-like fluctuation is observed to some extent. It is better to choose large q to investigate the pure nature of a first-order transition. But the amount of computation for equilibration becomes larger with increasing q. Typical spin configurations are shown in Fig. 1.

III. METHOD

We perform the Wang-Landau sampling simulations [17,18], which yield the density (number) of states $g(E)$, as a result of a learning process to realize a flat energy histogram. The density of states enables us to calculate the Helmholtz's free energy in canonical ensemble as $F(\beta) = \beta^{-1} \ln[\sum_E g(E) e^{-\beta E}]$, and its derivatives, i.e., mean energy and specific heat. The energy with maximum or minimum realization probability is given as a solution of $\partial[g(E)e^{-\beta E}]/\partial E = 0$, i.e., $\partial \ln g(E)/\partial E = \beta$.

On the other hand, in a microcanonical ensemble for given internal energy, a fundamental thermodynamic function is microcanonical entropy $S(E) = k_B \ln g(E)$, and (inverse) microcanonical temperature is a quantity to be observed, which is defined as a response to an energy perturbation as

$$\beta(E) = \frac{1}{k_B} \frac{\partial S(E)}{\partial E} = \frac{\partial}{\partial E} \ln g(E). \tag{2}$$

This is equivalent to the extremal condition for the free energy in a canonical ensemble. The E dependence of β in a microcanonical ensemble is not exactly related to the β dependence of *expectation* value of E in a canonical ensemble except in the thermodynamic limit but is exactly related to the β dependence of the *extremal* value of E even in the finite-size system.

We perform parallel computation to treat a large-size system as done in Ref. [18]. The energy region is divided into a number of parts with constant width, and each part is associated to a different thread. The spin flip trials that make the energy of the system go out of the given range is always rejected. Since the time needed to diffuse over the energy range ΔE by a random walk is proportional to ΔE^2, the time needed to obtain the flat histogram is inversely proportional to the square of the number of threads. Although this method drastically reduces the total Monte Carlo steps (MCSs), we have to care about the possibility that a flat histogram is established in MCSs shorter than the relaxation time of the system. This occurs when the energy region is divided into too small parts. Another problem of the division of the energy region is that it possibly causes the segmentation of the phase space; i.e., there are spin configurations that cannot be visited depending on the initial condition.

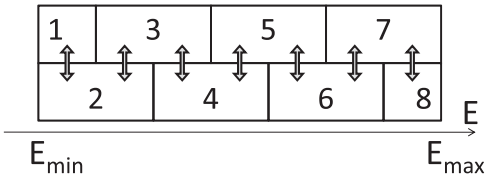

FIG. 2. Schematic diagram of dividing the energy region into eight threads and spin configuration exchange.

In order to enhance the relaxation and guarantees ergodicity, we make an overlapping energy region for neighboring threads as illustrated in Fig. 2, where exchange of spin configurations is allowed, satisfying a detailed balance condition:

$$\frac{W(\{X,Y\} \to \{Y,X\})}{W(\{Y,X\} \to \{X,Y\})} = \frac{g_i(E(X))g_j(E(Y))}{g_i(E(Y))g_j(E(X))},$$

where X and Y are indices of microscopic states, in the same spirit with the replica exchange method [19]. Here g_i is a density of states calculated by the ith thread, and $W(\{X,Y\} \to \{Y,X\})$ means the transition probability from a compound state: X for the ith thread and Y for the jth thread, to its exchanged state. Practically the exchange is accepted with a probability, $W(\{X,Y\} \to \{Y,X\}) = \min\{1, g_i[E(Y)]g_j(E(X))/g_i[E(X)]g_j[E(Y)]\}$, similarly with the Metropolis method.

In order to check the efficiency of the replica exchange method, the sample-to-sample deviations of temperature, $\delta\beta \equiv \sqrt{\overline{\beta^2} - |\overline{\beta}|^2}$, where $\overline{\cdots}$ means average over samples, are shown in Fig. 3. The conditions of simulations are described in its caption. The peaks are observed in the system without exchange. The amplitudes of the peaks become smaller as the exchange frequency increases. The peaks exist at the seam points, which are the edges of the divided region. Except around the seam points, the reduction of fluctuations is moderate. This is because the present system does not exhibit large fluctuation for a microcanonical state. The improvement by the exchange will be more remarkable for the system with a more complicated landscape in phase space.

IV. RESULTS

We perform a simulation with $q = 8$ and 21 for system size $L = 32$–1024 by using 4–64 threads. The density of states is calculated not for all energy regions but for a restricted region of interest. The numerical data shown below are averaged over 2–8 samples with different realizations of the random number.

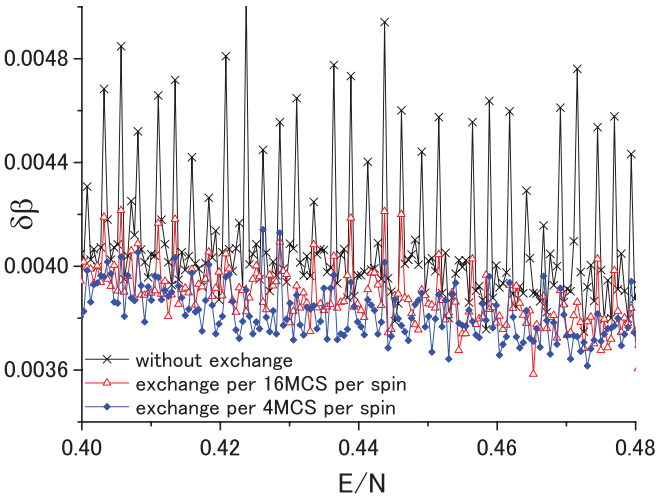

FIG. 3. (Color online) The standard deviation of microcanonical temperature among samples with different realizations of random number. The data without exchange and exchanges in every 16 and 4 MCSs per spin are plotted together. The simulation condition is $q = 8$, $L = 512$, 16 samples, and the modification constant is down to $\ln g(E) = 2^{-20}$. The energy region, $0.36 < E < 0.56$, is distributed to 64 threads, and each thread handles the energy points about 666×2. Smoothing is done by averaging for 128 energy points after calculating deviation. For comparison, the difference between the transition temperature and the spinodal temperature, a characteristic scale of our interest, is about 0.001 for this size, as shown in Fig. 4(a).

In the Wang-Landau sampling we decrease the modification constant for $\ln g(E)$ step by step, $1, 2^{-1}, 2^{-2}, \ldots, 2^{-30}$ (except for $q = 8$ with $L = 1024$ and $q = 21$ with $L = 512$, where the modification constant is decreased down to 2^{-25}) with achieving 90% flatness of energy histogram for all threads in every step. The typical number of total MCSs is 10^6–10^7 per spin in the final step of simulations. The replica exchange is attempted in every 16 MCSs per spin.

A. Temperature versus internal energy characteristics

Figure 4 shows the inverse microcanonical temperature $\beta(E) = \ln g(E+1) - \ln g(E)$ for $q = 8$ and 21 for various system size. While $\beta(E)$ should be a monotonically decreasing function of E to make the free energy a convex function of E, it is not for the finite-size system. In the region with positive derivative, i.e., negative specific heat, phase coexisting is observed as shown in Fig. 1. This state corresponds to the free-energy maximum in the canonical ensemble. A dip and a peak exist inside the coexisting region in the thermodynamic limit, $\varepsilon_c^- < E/N < \varepsilon_c^+$, where $\varepsilon_c^- \sim 0.403$ and $\varepsilon_c^+ \sim 0.888$ for $q = 8$ and $\varepsilon_c^- \sim 0.171$ and $\varepsilon_c^+ \sim 1.392$ for $q = 21$. We note the bottom (top) position of the dip (peak) as $(E,\beta) = [E_{\rm spi}^-(L), \beta_{\rm spi}^-(L)]$ and $[E_{\rm spi}^+(L), \beta_{\rm spi}^+(L)]$, respectively. These points are regarded as the equilibrium spinodal points, i.e., saddle-node bifurcation points, where the second free-energy minimum in canonical distribution annihilates together with the free-energy maximum. With increasing system size, $E_{\rm spi}^\pm/N$ approaches $\varepsilon_c^\pm$ and β approaches β_c for all E with $\varepsilon_c^- \leqslant E/N \leqslant \varepsilon_c^+$.

For $q = 21$, a plateau, where β almost equals β_c, is obviously observed in the middle of coexisting region. In this

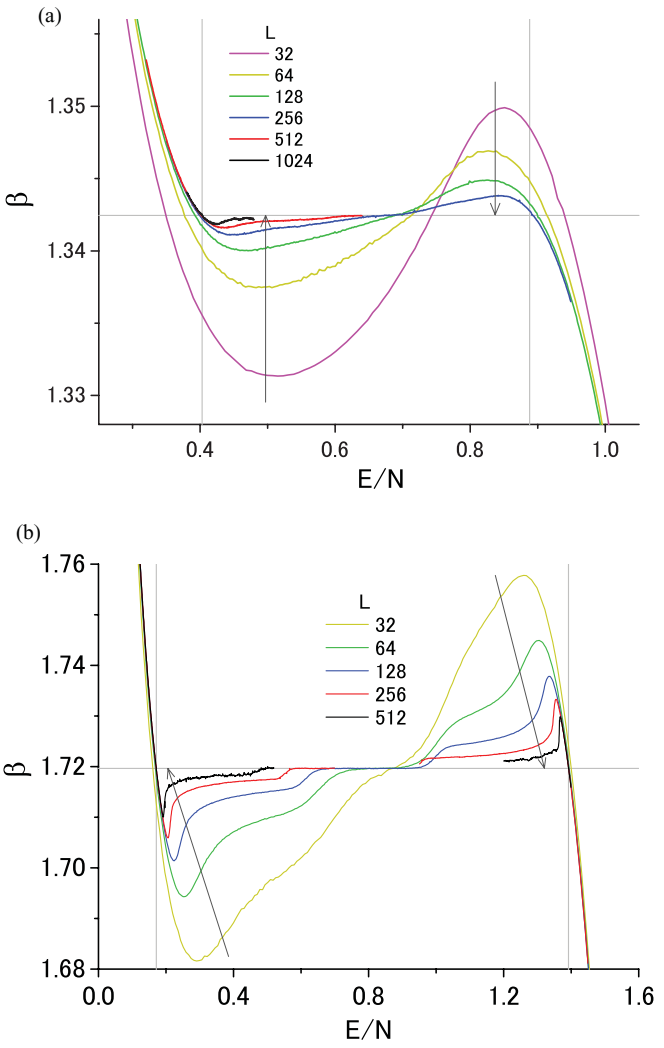

FIG. 4. (Color online) Inverse temperature as a function of internal energy for (a) $q = 8$ and (b) $q = 21$. Smoothing is performed by averaging over the range $\sqrt{N}/4$ of E. The horizontal line indicates $\beta = \ln(1 + 1/\sqrt{q})$. The vertical lines indicate $E/N = \varepsilon_c^-$ (left) and ε_c^+ (right). The arrows indicate the direction that L becomes larger.

plateau region, the two coexisting phases form strips parallel to the horizontal or longitudinal axis, while the minority phase forms a droplet in the side regions (Fig. 1). With increasing system size, it is observed that the plateau region becomes wider, and the steplike change of $\beta(E)$ on the edge becomes sharper as a consequence of the droplet-strip (slab) transition [10].

With increasing system size, the two spinodal points, $[E_{\rm spi}^\pm(L), \beta_{\rm spi}^\pm(L)]$, approach $(E_c^\pm, \beta_c) \equiv (N\varepsilon_c^\pm, \beta_c)$, respectively. The deviation $|\beta_{\rm spi}^\pm(L) - \beta_c|$ and $|E_{\rm spi}^\pm(L) - E_c^\pm|$ decreases as a power function of L [20]. To show it clearly, we perform finite-size scaling in Fig. 5 with expectation in a formula:

$$|\beta(E) - \beta_c| = L^{-d/(d+1)} F\left(\frac{|E - E_c^\pm|}{L^{d^2/(d+1)}}\right), \qquad (3)$$

with a scaling function $F(\cdot)$. The formula for the isotherm lattice gas model is derived in Ref. [5], where β and E are replaced with magnetic field and magnetization, respectively.

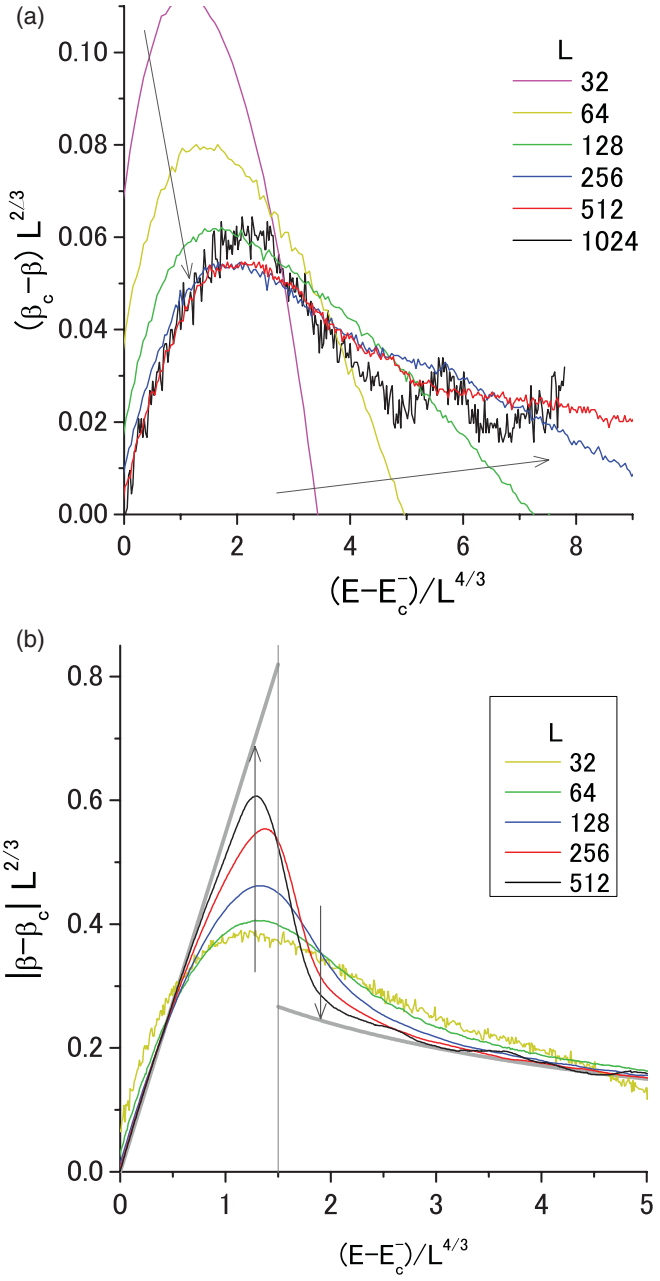

FIG. 5. (Color online) Finite-size scaling results of the excess temperature. (a) $q = 8$ and (b) $q = 21$. The arrows indicate the direction that L becomes larger. The thick gray curve is a guide for the eye. The vertical line in the bottom panel indicates $E - E_c^- = 1.507L^{4/3}$ as well as in Fig. 8.

For $q = 21$, it is observed that the scaled curve approaches a large-size limit; $|\beta - \beta_c|$ linearly increases as $(k_B\beta_c^2/C^{\pm})$ $|E - E_c^{\pm}|$, where $C^{\pm}$ is a specific heat $-k_B\beta^2[d^2 \ln g(E)/dE^2]^{-1}$ at $E = E_c^{\pm}$ in the evaporation phase, and discontinuously drops when entering the condensation phase. Note that this scaling does not target the collapse of data to a universal curve as in standard finite-size scaling for second-order transitions, but it is intended to show the conversion to the large-size limit by blowing up the transition region, which vanishes in macroscopic scale. (Scaling of finite-size rounding may be a challenging problem.) On the other hand, discontinuous behavior is rarely observed yet in the system with $q = 8$ even for $L = 1024$. This is because correlation length is rather large, and the used sample size is effectively much smaller than that for $q = 21$.

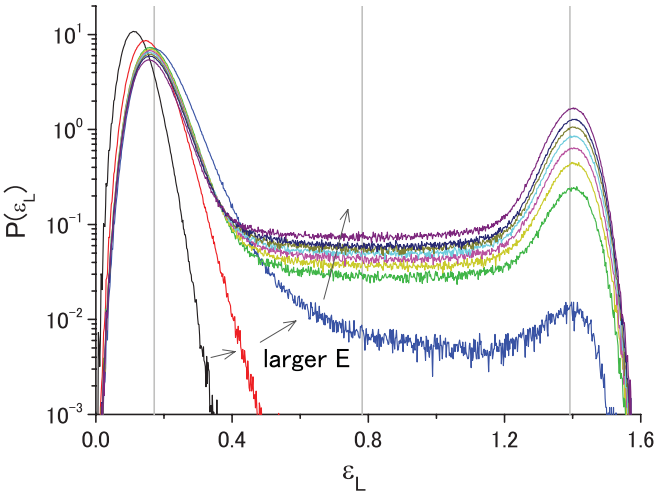

FIG. 6. (Color online) Probability distribution function of the energy density of subsystems for $q = 21$, $L = 512$. Each curve corresponds to $E/N = 0.12$–0.52 (0.02 step).

B. Volume fraction of a droplet

To observe the nature of droplet formation more directly, we evaluate the ratio of condensation volume to the whole system volume. To this end, we divide a sample into L square-shaped subsystems with size $\sqrt{L} \times \sqrt{L}$ ($\sqrt{L}$ is approximated by the closest integer if necessary). This resolution is fine enough to capture the shape of the critical droplet with a size of $O(L^{d^2/(d+1)})$. We calculate energy per spin ε_L for each square, whose distribution function $P(\varepsilon_L)$ is shown in Fig. 6. Hereafter we show only the results for $q = 21$. Bimodal distribution is observed in the condensed regime, $E_{\rm spi}^-(L) < E < E_{\rm spi}^+(L)$. The width of peaks becomes narrower as $\sqrt{\varepsilon_L L}/L \sim L^{-1/2}$, and the integral of bridge component between the two peaks corresponding to the perimeter of the droplet becomes smaller with $(2\pi L \times \sqrt{L})/N = L^{-1/2}$. The positions of the peaks hardly change with E, but only heights change for $E_{\rm spi}^-(L) < E < E_{\rm spi}^+(L)$, which means that the change of state in this regime can be described only by the change of mixing ratio of the two phases. We determine a subsystem with energy below (above) $\varepsilon_m = (\varepsilon_c^+ + \varepsilon_c^-)/2 = (1 - 1/\sqrt{q})$ [16] belongs to the ferro (para) domain.

The volume fraction of the para phase, $P(\varepsilon_L > \varepsilon_m)$, is plotted in Fig. 7. In the thermodynamic limit, $P(\varepsilon_L > \varepsilon_m)$ equals zero for $E \leqslant E_c^-$, unity for $E \geqslant E_c^+$, and linearly increases in between as $(E - E_c^-)/(E_c^+ - E_c^-)$. Finite-size deviation is observed on the edge of the coexisting region as shown in the insets of Fig. 7. The fraction of condensed phase for a finite-size system is smaller than that for $L = \infty$. The normalized condensation ratio

$$\lambda \equiv \frac{P(\varepsilon_L > \varepsilon_m)}{(E - E_c^-)/(E_c^+ - E_c^-)} \leqslant 1 \qquad (4)$$

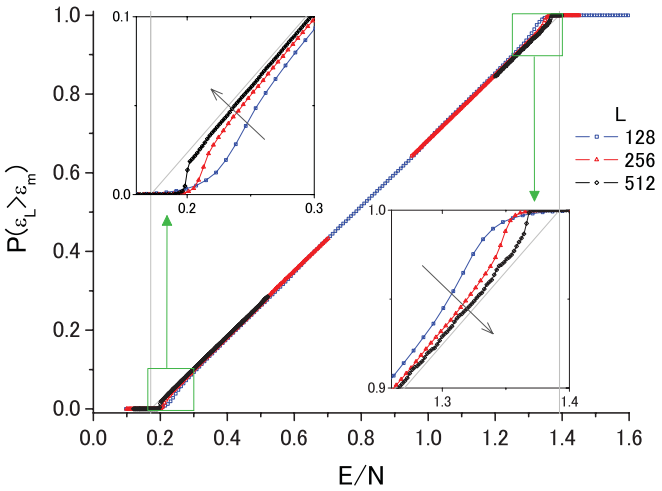

FIG. 7. (Color online) Internal energy dependence of the volume fraction of the high-energy domain. The insets are the blowups of the edges of the coexisting phase, where the arrows indicate the direction that L becomes larger.

is expected to be a function of a dimensionless variable:

$$\Delta = a\frac{(E - E_c^-)^{(d+1)/d}}{L^d} \tag{5}$$

$$\text{with} \quad a = \frac{\beta_c(\varepsilon_+ - \varepsilon_-)^{(d-1)/d}}{2C^-\tau_W} \tag{6}$$

for $L \to \infty$. Here τ_W is an interface free energy per volume of an optimally shaped large Wulff droplet [21]. The derivation of this formulas is described in Appendix. The behavior in the thermodynamic limit is exactly known [4] as $\lambda = 0$ for $\Delta < \Delta_c \equiv (1/2)(3/2)^{3/2}$ and $1/4\sqrt{\lambda}(1-\lambda) = \Delta$ for $\Delta > \Delta_c$. While C^- is estimated as 5.41, τ_W is the only unknown quantity needed to calculate Δ. By only assuming $\tau_W = 0.40$ (then $a = 0.44$), however, our numerical result shows good agreement with theory as shown in Fig. 8. While λ decreases to zero with increasing L for $\Delta < \Delta_c$, very little finite-size dependence is observed, $\Delta > \Delta_c$. The gap of λ at Δ_c also coincides with the predicted value $2/3$.

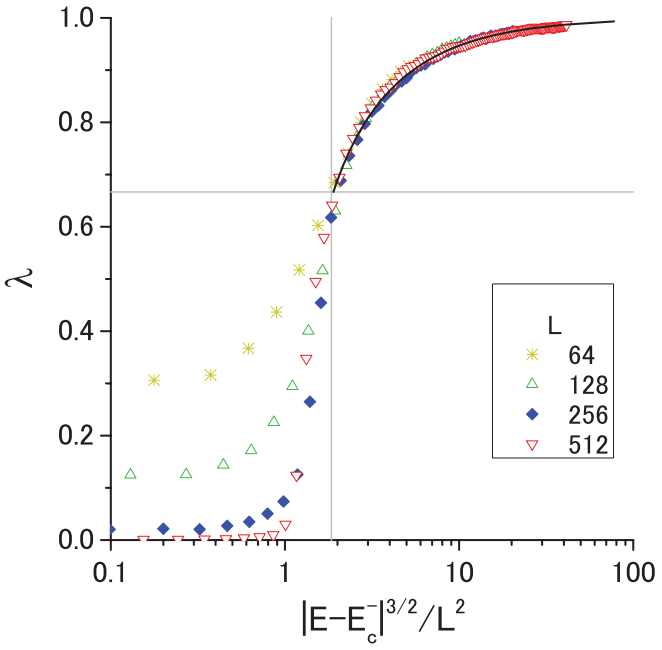

FIG. 8. (Color online) Finite-size scaling result of the volume fraction of a condensed droplet. The data for $E/N < 0.40$ are used. The solid gray curve indicates theoretical prediction, $a|E - E_c^-|^{3/2}/L^2 = 1/4\sqrt{\lambda}(1-\lambda)$ for $\lambda > 2/3$, where we set $a = 0.44$. The vertical line indicates $E - E_c^- = 1.507L^{4/3}$ as well as in Fig. 5.

V. CONCLUSION

We have investigated the condensation-evaporation transition of the Potts model in microcanonical ensemble. Interesting property of this transition is that it becomes impossible to be found in the true thermodynamic limit; the width of the supersaturation regime disappears, but discontinuity of scaled quantities becomes clear with increasing system size. The present numerical results with $q = 21$ show good agreement with the theoretical prediction of the system-size dependence both for temperature [5] and for the condensation ratio [4]. Both of them mean that a droplet with size smaller than $O(L^{d^2/(d+1)})$ is unstable.

For a finite-size system in a microcanonical ensemble, we observe negative (inverse) specific heat in the coexisting region and over- or under-hang of temperature, which corresponds to the thermodynamic spinodal point in a canonical ensemble. The scaling behavior $|\beta_{\rm spi} - \beta_c| \propto L^{-d/(d+1)}$ suggests an existence of a diverging length scale, $R_s(\beta) \propto |\beta - \beta_c|^{-(d+1)/d}$. This means that a supersaturation state at given temperature β becomes unstable at a length scale above R_s. Although this length is related to the equilibrium spinodal point, it is not clear whether it also has some meanings in nonequilibrium dynamics, which may be an interesting open problem.

Last, let us note the difficulty of the simulation of first-order transitions. We suffered from slow relaxation for large system size in the present study as well as that discussed in Ref. [10]. It is considered that the Wang-Landau sampling is quite efficient for first-order transitions with discontinuity $O(L^d)$ as well as some other extended ensemble methods, such as the multicanonical method [22], because it provides additional probability weight on coexisting states to bridge the divide between two distinct homogeneous states, such as para and ferro phases. However, there are still discontinuous transitions in the coexisting phase, that is, a evaporation-condensation transition with $O(L^{d^2/(d+1)})$ discontinuity and droplet-slab transition [10,11]. This behavior is general for first-order transitions. Since the problem is that the two states are energetically degenerate in these transitions, one fundamental solution to this problem may be to employ another argument that corresponds to the shape of domains for the joint density of state [18,23]. Although it requires a considerable amount of computation, massive parallel computation makes it feasible.

ACKNOWLEDGMENT

This work was partly supported by Award No. KUK-I1-005-04 made by King Abdullah University of Science and Technology (KAUST).

APPENDIX: FINITE-SIZE EFFECT ON DROPLET CONDENSATION RATIO

Here we derive the condensation rate of a droplet for a energy-driven phase transition by translating the result for a magnetization-driven transition [4,13]. We consider a canonical ensemble at the bistable point $\beta = \beta_c$ and its energy distribution function around a peak at E_c^-. (The case around the other peak E_c^+ is derived in the same way.)

We note the excess energy in fluctuation beyond the peak as $\delta E = E - E_c^-$ and divide it into two parts, $\delta E = \delta E_b + \delta E_d$, where δE_b is due to small bubble excitation and δE_d is due to a large droplet of disordered phase. If introducing the condensation ratio λ as $\delta E_d \equiv \lambda \delta E$, the rest is given by $\delta E_b = (1-\lambda)\delta E$. The volume of the droplet, $V_d \equiv \lambda V_L$, can be smaller than that in the thermodynamic limit, $V_L = \delta E/(\varepsilon_c^+ - \varepsilon_c^-)$, for a finite-size system. By using these quantities, the energy distribution function $P(\beta_c; E)$ is proportional to $e^{-\beta_c F}$, where

$$F = \frac{\beta_c(\delta E_b)^2}{2L^d C^-} + \tau_W V_d^{(d-1)/d} \tag{A1}$$

$$= \tau_W V_L^{(d-1)/d}[\Delta(1-\lambda)^2 + \lambda^{(d+1)/d}] \tag{A2}$$

$$\text{with} \quad \Delta \equiv \frac{\beta_c(\varepsilon_c^+ - \varepsilon_c^-)^{(d-1)/d}}{2C^-\tau_W}\frac{(\delta E)^{(d+1)/d}}{L^d}. \tag{A3}$$

The first term indicates the fluctuation without phase coexistence characterized by specific heat C^-, and the second term indicates the surface free energy of a large droplet.

The condensation rate λ depends only on the dimensionless parameter Δ, which is related to the excess energy. For given Δ, free energy F is minimized at

$$\lambda = 0 \quad \text{for} \quad \Delta \leqslant \Delta_c \equiv (1/2)(3/2)^{3/2}, \tag{A4}$$

which means a supersaturation regime, while λ for minimum F is given by a solution of

$$1/4\sqrt{\lambda}(1-\lambda) = \Delta \quad \text{for} \quad \Delta \geqslant \Delta_c, \tag{A5}$$

which means a condensation regime. The two states with $\lambda = 0$ and $\lambda \equiv \lambda_c = 2/3$ are equivalently stable at Δ_c.

This discontinuous change at Δ_c is directly observed as an internal energy-driven transition in microcanonical ensemble.

[1] P. A. Rikvold, H. Tomita, S. Miyashita, and S. W. Sides, Phys. Rev. E **49**, 5080 (1994).
[2] M. A. Novotny, G. Brown, and P. A. Rikvold, J. App. Phys. **91**, 6908 (2002).
[3] B. A. Berg and S. Dubey, Phys. Rev. Lett. **100**, 165702 (2008).
[4] M. Biskup, L. Chayes, and Kotecký, Europhys. Lett. **60**, 21 (2002).
[5] K. Binder, Physica A **319**, 99 (2003).
[6] K. Binder and M. H. Kalos, J. Stat. Phys. **22**, 363 (1980).
[7] L. G. MacDowell, P. Virnau, M. Müller, and K. Binder, J. Chem. Phys. **120**, 5293 (2004).
[8] L. G. MacDowell, V. K. Shen, and J. R. Errington, J. Chem. Phys. **125**, 034705 (2006).
[9] M. Schrader, P. Virnau, and K. Binder, Phys. Rev. E **79**, 061104 (2009).
[10] T. Neuhaus and J. S. Hager, J. Stat. Phys. **113**, 1 (2003).
[11] A. Nußbaumer, E. Bittner, T. Neuhaus, and W. Janke, Europhys. Lett. **75**, 716 (2006).
[12] S. S. Martinos, A. Malakis, and I. Hadjiagapiou, Physica A **384**, 368 (2007).
[13] A. Nußbaumer, E. Bittner, T. Neuhaus, and W. Janke, Prog. Theor. Phys. Suppl. **184**, 400 (2010).
[14] D. H. E. Gross, A. Ecker, and X. Z. Zhang, Ann. Phys. **508**, 446 (1996).
[15] W. Janke, Nucl. Phys. B, Proc. Suppl. **63**, 631 (1998).
[16] F. Y. Wu, Rev. Mod. Phys. **54**, 235 (1982).
[17] F. Wang and D. P. Landau, Phys. Rev. Lett. **86**, 2050 (2001).
[18] D. P. Landau, S.-H. Tsai, and M. Exler, Am. J. Phys. **72**, 1294 (2004).
[19] K. Hukushima and K. Nemoto, J. Phys. Soc. Jpn. **65**, 1604 (1996).
[20] A. Bazavov, B. A. Berg, and S. Dubey, Nuc. Phys. B **802**, 421 (2008).
[21] G. Wulff and Z. Kristallogr, Mineral. **34**, 449 (1901).
[22] B. A. Berg and T. Neuhaus, Phys. Rev. Lett. **68**, 9 (1992).
[23] C. Zhou, T. C. Schulthess, S. Torbrügge, and D. P. Landau, Phys. Rev. Lett. **96**, 120201 (2006).